



RELAXATION SOLVERS FOR IDEAL MHD EQUATIONS -A REVIEW*

Dedicated to Professor James Glimm on the occasion of his 75th birthday

Christian Klingenberg

Department of Mathematics, Würzburg University, Am Hubland 97074 Würzburg, Germany

E-mail: klingenberg@mathematik.uni-wuerzburg.de

Knut Waagan

The University of Maryland, CSCAMM, 4146 CSIC Building #406 Paint Branch Drive,

College Park MD 20742-3289, USA

E-mail: kwaagan@cscamm.umd.edu

Abstract We have developed approximate Riemann solvers for ideal MHD equations based on a relaxation approach in [4], [5]. These lead to entropy consistent solutions with good properties like guaranteed positive density. We describe the extension to higher order and multiple space dimensions. Finally we show our implementation of all this into the astrophysics code FLASH.

Key words conservation laws; ideal magnetohydrodynamics; finite volume schemes; entropy stable schemes; positive schemes

2000 MR Subject Classification 35L65; 65M08

1 Introduction

In this paper we study finite volume methods for the equations of ideal MHD. We derive approximate Riemann solvers based on a relaxation approach. For the Euler equations of compressible fluids this relaxation approach is well described in the book of Francois Bouchut [3] and references therein. The generalisation of this to ideal MHD is described in [4], [5] which we review below.

The MHD system (letting I_3 denote the 3×3 identity matrix)

$$\begin{aligned}\rho_t + \nabla \cdot (\rho \mathbf{u}) &= 0, \\ (\rho \mathbf{u})_t + \nabla \cdot (\rho \mathbf{u} \otimes \mathbf{u} + (p + \frac{1}{2} |\mathbf{B}|^2) I_3 - \mathbf{B} \otimes \mathbf{B}) &= 0, \\ E_t + \nabla \cdot [(E + p + \frac{1}{2} |\mathbf{B}|^2) \mathbf{u} - (\mathbf{B} \cdot \mathbf{u}) \mathbf{B}] &= 0, \\ \mathbf{B}_t + \nabla \cdot (\mathbf{B} \otimes \mathbf{u} - \mathbf{u} \otimes \mathbf{B}) &= 0, \\ \nabla \cdot \mathbf{B} &= 0,\end{aligned}\tag{1.1}$$

*Received March 12, 2010.

with an internal energy e given by $E = \rho e + \frac{1}{2}\rho \mathbf{u}^2 + \frac{1}{2}\mathbf{B}^2$, and the pressure given by the equation of state $p = p(\rho, e)$. The system fits the generic form of a conservation law $U_t + \nabla \cdot \mathbf{F}(\mathbf{U}) = \mathbf{0}$, except for the restriction on $\nabla \cdot \mathbf{B}$. However, if this restriction is satisfied at the initial time $t = 0$, it automatically holds at later times $t > 0$ for the exact solution.

Thermodynamical considerations leads to the assumption of existence of a specific physical entropy $s = s(\rho, e)$ that satisfies

$$de + p d\left(\frac{1}{\rho}\right) = T ds \quad (1.2)$$

for some temperature $T(\rho, e) > 0$. To ensure the hyperbolicity of (2.1)–(2.5), we assume that

$$p' \equiv \left(\frac{\partial p}{\partial \rho}\right)_s > 0, \quad (1.3)$$

where the subscript s means that the partial derivative is taken with s constant. We shall also make the classical assumption that

$$-s \text{ is a convex function of } \left(\frac{1}{\rho}, e\right). \quad (1.4)$$

The system is then equipped with the entropy inequality

$$(\rho\phi(s))_t + (\rho u\phi(s))_x \leq 0 \quad (1.5)$$

in accordance with the second law of thermodynamics.

Consider a one-dimensional hyperbolic conservation law

$$U_t + F(U)_x = 0. \quad (1.6)$$

A conservative scheme for this system can be given by

$$U_{i,j}^{n+1} = U_{i,j}^n - \frac{\Delta t}{\Delta x} (\mathcal{F}_{i+\frac{1}{2},j}^n - \mathcal{F}_{i-\frac{1}{2},j}^n). \quad (1.7)$$

For a first order scheme, we set $\mathcal{F}_{i+\frac{1}{2},j}^n = \mathcal{F}(U_{i,j}^n, U_{i+1,j}^n)$, where $\mathcal{F}(\cdot, \cdot)$ is typically given by an exact or an approximate Riemann solver.

2 The Relaxation Approach in One Dimension

The equations for ideal MHD in one dimension are

$$\rho_t + (\rho u)_x = 0, \quad (2.1)$$

$$(\rho u)_t + (\rho u^2 + p + \frac{1}{2}|B_\perp|^2 - \frac{1}{2}B_n^2)_x = 0, \quad (2.2)$$

$$(\rho u_\perp)_t + (\rho u u_\perp - B_n B_\perp)_x = 0, \quad (2.3)$$

$$E_t + [(E + p + \frac{1}{2}|B_\perp|^2 - \frac{1}{2}B_n^2)u - B_n(B_\perp \cdot u_\perp)]_x = 0, \quad (2.4)$$

$$(B_\perp)_t + (B_\perp u - B_n u_\perp)_x = 0. \quad (2.5)$$

The velocity is split into its longitudinal and transverse components u and u_\perp , and the magnetic field similarly into B_n and B_\perp . Hence u_\perp and B_\perp are two-dimensional vectors. Since the

divergence of the magnetic field is zero at all times, we take B_n constant for one-dimensional data, but we will eventually need to relax that restriction.

2.1 Relaxation system and approximate Riemann solver

In [4] we introduced the relaxation system

$$\begin{aligned}
 \rho_t + (\rho u)_x &= 0, \\
 (\rho u)_t + (\rho u^2 + \pi)_x &= 0, \\
 (\rho u_\perp)_t + (\rho u u_\perp + \pi_\perp)_x &= 0, \\
 E_t + [(E + \pi)u + \pi_\perp \cdot u_\perp]_x &= 0, \\
 (B_\perp)_t + (B_\perp u - B_n u_\perp)_x &= 0
 \end{aligned}
 \tag{2.6}$$

with $E = \rho e + \frac{1}{2}\rho u^2 + \frac{1}{2}\mathbf{B}^2$, and where the relaxation pressures π and π_\perp evolve according to

$$\begin{aligned}
 (\rho \pi)_t + (\rho \pi u)_x + (|b|^2 + c_b^2)u_x - c_a b \cdot (u_\perp)_x &= 0, \\
 (\rho \pi_\perp)_t + (\rho \pi_\perp u)_x - c_a b u_x + c_a^2 (u_\perp)_x &= 0.
 \end{aligned}
 \tag{2.7}$$

The parameters $c_a \geq 0$, $c_b \geq 0$, and $b \in \mathbf{R}^2$ play the role of approximations of $\sqrt{\rho}|B_n|$, $\rho\sqrt{p'}$ and $\text{sign}(B_n)\sqrt{\rho}B_\perp$ respectively. Indeed, c_a, c_b, b are not taken constant, but are evolved with

$$(c_a)_t + u(c_a)_x = 0, \quad (c_b)_t + u(c_b)_x = 0, \quad b_t + u b_x = 0.
 \tag{2.8}$$

We can refer to

$$\pi = p + \frac{1}{2}|B_\perp|^2 - \frac{1}{2}B_x^2 \quad \text{and} \quad \pi_\perp = -B_x B_\perp.
 \tag{2.9}$$

as an equilibrium state. The approximate Riemann solver results from projecting the solution to the equilibrium state at discrete times, while also computing cell averages.

The eigenvalues of the system (2.6), (2.7) and (2.8) are $u, u \mp \frac{c_s}{\rho}, u \mp \frac{c_a}{\rho}$ and $u \mp \frac{c_f}{\rho}$, where

$$\begin{aligned}
 c_s^2 &= \frac{1}{2}(c_b^2 + c_a^2 + |b|^2 - \sqrt{(c_b^2 + c_a^2 + |b|^2)^2 - 4c_a^2 c_b^2}), \\
 c_f^2 &= \frac{1}{2}(c_b^2 + c_a^2 + |b|^2 + \sqrt{(c_b^2 + c_a^2 + |b|^2)^2 - 4c_a^2 c_b^2}),
 \end{aligned}
 \tag{2.10}$$

u having multiplicity 8. All are linearly degenerate, hence the Riemann problem is easy to solve. Note that $c_s \leq c_a \leq c_f$, $c_s \leq c_b \leq c_f$, and that the eigenvalues of (2.6), (2.7) and (2.8) equal the eigenvalues of (2.1)-(2.5) whenever $c_a = \sqrt{\rho}|B_n|$, $c_b = \rho\sqrt{p'}$ and $b = \text{sign}(B_n)\sqrt{\rho}B_\perp$. However, in order to simplify, we shall make here different choices, leading to a solver with 3 waves or 5 waves instead of 7 waves. The full motivation and analysis of the relaxation system is given in [4]. We get conditions to ensure that for a Riemann problem starting at equilibrium (2.9), the solution to the relaxation system satisfies: (i) the mass density stays positive, and (ii) The entropy inequality (1.5) holds. As a consequence, we get a scheme of form (1.7) such that mass density and internal energy stays positive, and the following discrete entropy inequality holds:

$$\eta(U_i^{n+1}) - \eta(U_i^n) + \frac{\Delta t}{\Delta x}[G^c(U_i^n, U_{i+1}^n) - G^c(U_{i-1}^n, U_i^n)] \leq 0,
 \tag{2.11}$$

with $\eta(U) = \rho\phi(s(\rho, e))$, and G^c an appropriate numerical entropy flux.

The stability conditions for the approximate Riemann solver are given as inequalities involving c_b , c_a and b , and the solution of the relaxation system. Since the Riemann problem solution is explicit, we can obtain explicit values of c_b , c_a and b that ensure good properties.

The simplest choice is to take $b = 0$ and $c = c_a = c_b$. The resulting Riemann solver has three distinct wave speeds. Fast waves, material contact waves and tangential discontinuities are resolved sharply by this solver. We also observe good resolution of other waves in practice. In order to allow optimal resolution of velocity shear waves when B_n vanishes, we also provide a 5-wave solver where still $b = 0$, and c_a is independent of c_b in such a way that it vanishes with B_n .

2.2 Second order accuracy

Let $U^\pm = U \pm \frac{1}{2}DU$, where $\frac{DU}{\Delta x}$ is a second order accurate approximation to U_x . Then the MUSCL scheme

$$U_i^{n+1} = U_i^n - \frac{\Delta t}{\Delta x} (\mathcal{F}(U_i^+, U_{i+1}^-) - \mathcal{F}(U_{i-1}^+, U_i^-)) \quad (2.12)$$

is second order accurate in space. Second order accuracy in time can be achieved by Heun's method. One can also use a predictor-corrector type scheme to restore time accuracy, for example in the MUSCL-Hancock scheme, where one takes $U^\pm = U \pm \frac{1}{2}DU + \frac{1}{2}\Delta t F'(U)DU$. A stable MUSCL-Hancock scheme is presented in [18]. For brevity, we stick to the MUSCL scheme with $U^\pm = U \pm \frac{1}{2}DU$ here, the stability results of which are a special case in [18].

The first step in making (2.12) stable is to follow [17] and limit the gradient DU . This approach is inspired by the total variation diminishing property of scalar conservation laws, suggesting that the reconstructed state, represented by U^\pm , should not have a larger total variation than the original state U . One may also use the ENO ([12]) or WENO ([16]) approaches, based on similar principles, to find U^\pm . It is not necessary to base the reconstruction on a piecewise linear approximation to the conserved quantities. Instead, we will consider piecewise linear approximations to the primitive variables $W = (\rho, \mathbf{u}, \mathbf{B}, p)$. For our numerical examples, we employ the monotonized central limiter

$$DW_i = \sigma_i \min \left(2|W_{i+1} - W_i|, \frac{1}{2}|W_{i+1} - W_{i-1}|, 2|W_i - W_{i-1}| \right) \quad (2.13)$$

with

$$\sigma_i = \begin{cases} 1, & W_{i+1} - W_i > 0, W_i - W_{i-1} > 0, \\ -1, & W_{i+1} - W_i < 0, W_i - W_{i-1} < 0, \\ 0, & \text{otherwise.} \end{cases} \quad (2.14)$$

In the above formulas, minimization and absolute value are to be understood as component-wise operations on each scalar quantity of W_i .

Next, we would like the positivity and entropy stability of the first order scheme to hold also for (2.12). It turns out to not be very practical to use a provably entropy stable scheme for higher order. Instead, we rely on the gradient limiting to force the scheme towards its first order version near shocks, hence ensuring sufficient dissipation. Positivity, on the other hand, can only be ensured if some additional limiting is performed. We rely on the following result (See [18], Prop. 3.2):

Proposition 2.1 The scheme (2.12) is positive if

$$|D\rho| < 2\rho, \quad |Dp| < 2p \quad (2.15)$$

and

$$\left(\rho + \frac{D\rho^2}{2\rho}\right)D\mathbf{u}^2 + D\mathbf{B}^2 < 4\rho e. \tag{2.16}$$

Note that the relations (2.15) follow from (2.13), and more generally hold for any reconstruction such that (for each component of W)

$$W^\pm \geq \min_i W_i.$$

The last inequality (2.16) can be imposed by taking a gradient DW from e.g. (2.13), and replacing it with

$$\sqrt{\frac{4\rho e}{\max\left(\left(\rho + \frac{D\rho^2}{2\rho}\right)D\mathbf{u}^2 + D\mathbf{B}^2, 4\rho e\right)}} DW.$$

Numerical tests in [18] validates the use of Prop 2.1.

3 Multidimensions

The ideal MHD equations (1.1) consists of a system of conservation laws, and the divergence constraint $\nabla \cdot \mathbf{B} = 0$. Taking the divergence of the evolution equation for \mathbf{B} , yields that $(\nabla \cdot \mathbf{B})_t = 0$. Hence, the divergence constraint only needs to be imposed on the initial data. It is a nontrivial issue how to account for the divergence constraint in a numerical simulation, particularly in presence of the low regularity exhibited by solutions to ideal MHD.

In finite volume schemes for equations like (1.1), exact or approximate Riemann solvers for one-dimensional systems are crucial components also in multiple dimensions. As an example, consider in two space dimensions a Cartesian grid with cell centers (x_i, y_i) , and the system

$$U_t + F(U)_x + G(U)_y = 0. \tag{3.1}$$

A finite volume scheme for this system can be given by

$$U_{i,j}^{n+1} = U_{i,j}^n - \frac{\Delta t}{\Delta x} (\mathcal{F}_{i+\frac{1}{2},j}^n - \mathcal{F}_{i-\frac{1}{2},j}^n) - \frac{\Delta t}{\Delta y} (\mathcal{G}_{i,j+\frac{1}{2}}^n - \mathcal{G}_{i,j-\frac{1}{2}}^n). \tag{3.2}$$

For a first order scheme, the numerical flux $\mathcal{F}_{i+\frac{1}{2},j}^n$ is set as $\mathcal{F}(U_{i,j}^n, U_{i+1,j}^n)$, as in the one-dimensional scheme (1.7). The resulting scheme can be proved to preserve the stability properties of the basic one-dimensional scheme at the expense of lowering the CFL number by a factor of 2. Typically, such a reduction in the CFL number is not found necessary in practice.

In developing the approximate Riemann solver for one dimension, we assumed that B_n was constant due to the divergence constraint. On the other hand, when evaluating the numerical fluxes in (3.2), this is no longer true. A simple way to get around the problem is to use a local average of B_n to evaluate the flux. This technique can not be expected to preserve the stability properties of the Riemann solver. Instead, we will base the scheme on the Powell system [15], which means that the magnetic induction equation is rewritten as

$$\mathbf{B}_t + \nabla \cdot (\mathbf{B} \otimes \mathbf{u} - \mathbf{u} \otimes \mathbf{B}) = -\mathbf{u} \nabla \cdot \mathbf{B}. \tag{3.3}$$

Note that a nonconservative term proportional to $\nabla \cdot \mathbf{B}$ has been added. In [15], similar source terms were added to the momentum and energy equations, resulting in a symmetrizable system.

For our purpose it is sufficient to modify the induction equation. Taking the divergence of (3.3) yields

$$(\nabla \cdot \mathbf{B})_t + \nabla \cdot (\mathbf{u} \nabla \cdot \mathbf{B}) = 0. \quad (3.4)$$

This means that if $\nabla \cdot \mathbf{B} = 0$ initially, it remains so, and consequently the standard form (1.1) and the Powell system are equivalent. We also note that the entropy inequality (1.5) holds also for Powell's system. However, in the presence of small errors in the divergence constraint, the Powell system is stable, while the standard form is not. Furthermore, we are able to extend our stability results in one dimension to multi-dimensions via the Powell-terms approach.

3.1 First order

The next step is to describe how the relaxation system, and corresponding Riemann solver, can be extended to the Powell's system. The relaxation system for Powell's system only differs from the standard case (2.6)–(2.7) in the form (3.3) of the induction equation. The solution of the Riemann problem for the relaxation system with (3.3) is the same as before with the addition that B_n jumps from B_n^l to B_n^r across the middle wave. The resulting approximate Riemann solver satisfies the same entropy stability and positivity conditions as are valid for constant B_n .

The numerical fluxes for ρ , $\rho \mathbf{u}$ and E are calculated as before (with B_n evaluated locally), while the numerical fluxes for \mathbf{B} become non-conservative and are found in the following way: The approximate solution satisfies

$$\mathbf{B}_t + (\mathbf{B}u - B_n \mathbf{u})_x + \mathbf{u}(B_n)_x = 0. \quad (3.5)$$

Denote by u^* the value of u through the material contact. Then,

$$(B_n)_x = (B_n^r - B_n^l)\delta(x - tu^*), \quad \mathbf{u}(B_n)_x = \mathbf{u}^*(B_n^r - B_n^l)\delta(x - tu^*), \quad (3.6)$$

where \mathbf{u}^* is the value of \mathbf{u} through the material contact. We also have the jump condition

$$[\mathbf{B}u - B_n \mathbf{u}]_{x=0} + \mathbf{u}^*(B_n^r - B_n^l)\mathbf{1}_{u^*=0} = 0, \quad (3.7)$$

where $[\dots]_{x=0}$ denotes the jump through the line $x = 0$.

Now, integrate (3.5) over $(0, \Delta t) \times (-\Delta x, 0)$. We get

$$\begin{aligned} & \frac{1}{\Delta x} \int_{-\Delta x}^0 \mathbf{B}(x/\Delta t) dx - \mathbf{B}_l + \frac{\Delta t}{\Delta x} ((\mathbf{B}u - B_n \mathbf{u})_{0-} - (\mathbf{B}u - B_n \mathbf{u})_l) \\ & + \frac{\Delta t}{\Delta x} \mathbf{u}^*(B_n^r - B_n^l)\mathbf{1}_{u^*<0} = 0. \end{aligned} \quad (3.8)$$

Next, integrate (3.5) over $(0, \Delta t) \times (0, \Delta x)$. We get

$$\begin{aligned} & \frac{1}{\Delta x} \int_0^{\Delta x} \mathbf{B}(x/\Delta t) dx - \mathbf{B}_r + \frac{\Delta t}{\Delta x} ((\mathbf{B}u - B_n \mathbf{u})_r - (\mathbf{B}u - B_n \mathbf{u})_{0+}) \\ & + \frac{\Delta t}{\Delta x} \mathbf{u}^*(B_n^r - B_n^l)\mathbf{1}_{u^*>0} = 0. \end{aligned} \quad (3.9)$$

Denote

$$\begin{aligned} F_l^{\mathbf{B}} &= (\mathbf{B}u - B_n \mathbf{u})_{0-} + \mathbf{u}^*(B_n^r - B_n^l)\mathbf{1}_{u^*<0}, \\ F_r^{\mathbf{B}} &= (\mathbf{B}u - B_n \mathbf{u})_{0+} - \mathbf{u}^*(B_n^r - B_n^l)\mathbf{1}_{u^*>0}. \end{aligned} \quad (3.10)$$

We end up with

$$\mathbf{B}_i^{n+1} - \mathbf{B}_i^n + \frac{\Delta t}{\Delta x} ((F_l^{\mathbf{B}})_{i+1/2} - (F_r^{\mathbf{B}})_{i-1/2}) = 0. \tag{3.11}$$

According to (3.7), a formula for the numerical fluxes is

$$\text{If } u^* \geq 0 \text{ then } \begin{cases} F_l^{\mathbf{B}} = (\mathbf{B}u - B_n \mathbf{u})_{0-}, \\ F_r^{\mathbf{B}} = (\mathbf{B}u - B_n \mathbf{u})_{0-} - \mathbf{u}^*(B_n^r - B_n^l), \end{cases} \tag{3.12}$$

$$\text{If } u^* \leq 0 \text{ then } \begin{cases} F_l^{\mathbf{B}} = (\mathbf{B}u - B_n \mathbf{u})_{0+} + \mathbf{u}^*(B_n^r - B_n^l), \\ F_r^{\mathbf{B}} = (\mathbf{B}u - B_n \mathbf{u})_{0+}. \end{cases} \tag{3.13}$$

This completes the description of the first order multidimensional scheme of form (3.2). Note that when B_n is allowed to vary, the first order scheme (1.7) generalises to the form

$$U_i^{n+1} = U_i^n - \frac{\Delta t}{\Delta x} (\mathcal{F}_l(U_i, U_{i+1}) - \mathcal{F}_r(U_{i-1}, U_i)). \tag{3.14}$$

3.2 Second order extension

Following (2.12) and (3.14), it is tempting to take as a second order extension,

$$U_i^{n+1} = U_i^n - \frac{\Delta t}{\Delta x} (\mathcal{F}_l(U_i^+, U_{i+1}^-) - \mathcal{F}_r(U_{i-1}^+, U_i^-)). \tag{3.15}$$

However, this will not lead to a consistent scheme for the Powell system. Indeed, since the source term contribution from the flux at the cell edges is proportional to $B_n^r - B_n^l$, the contribution will formally vanish up to the truncation order of the reconstruction. We therefore follow [1] in adding a source contribution S , yielding

$$U_i^{n+1} = U_i^n - \frac{\Delta t}{\Delta x} (\mathcal{F}_l(U_i^+, U_{i+1}^-) - \mathcal{F}_r(U_{i-1}^+, U_i^-)) - \Delta t S_i^n. \tag{3.16}$$

The idea is to have S restore the order of accuracy. Near a discontinuity, the scheme goes to first order, in which case the source contributions from the flux are consistent, hence S should vanish. A simple choice fulfilling these criteria is given by

$$S_i = \left(0, 0, 0, 0, \mathbf{u}_i \frac{(DB_n)_i}{h}, 0 \right). \tag{3.17}$$

This was found to be a very robust choice in [18]. One can also find S such that positivity proofs are known. However, those choices were a little more expensive to calculate as they involved partially solving additional Riemann problems. We recommend using (3.17) as it appears to work equally well.

This way of discretising the Powell term is also studied in [10]. In contrast, it has been common to use central discretisation for the Powell term. For example, one may set,

$$S_i = \left(0, 0, 0, 0, \mathbf{u}_i \frac{(B_n)_{i+1} - (B_n)_{i-1}}{2h}, 0 \right), \tag{3.18}$$

and avoid the contribution from the cell edges (Either by using an average value of B_n , or by truncating the source contribution. The latter leads to a discontinuous flux).

4 Numerical Examples

We present a selection of numerical tests here. For more extensive testing, we refer the reader to [5] and [18]. In [5] the 3 and 5-wave solvers are extensively tested in one dimension. In [18] the applicability of our second-order and multidimensional approach is demonstrated. For the Euler equations, the relaxation solvers were tested in [13], which included three-dimensional turbulence problems. The second order accurate scheme has been implemented in the Flash code [19] which is an AMR (adaptive mesh refinement) code for astrophysical applications, see [9].

4.1 Brio-Wu shock tube

First we consider the standard shock tube test of [7]. It is considered a good test of a scheme's ability to deal with the complicated wave structure of ideal MHD. The initial data are given by $U = U_l$ for $x < 0.5$, and $U = U_r$ for $x > 0.5$, with $\gamma = 2$ and

$$\rho_l = 1, \mathbf{u}_l = 0, \mathbf{B}_l = (0.75, 1, 0), p_l = 1,$$

$$\rho_r = 0.125, \mathbf{u}_r = 0, \mathbf{B}_r = (0.75, -1, 0), p_r = 0.1.$$

Figure 4.1 shows the resulting ρ and B_y . The solution consists of, from left to right, a fast rarefaction, a compound wave, a contact discontinuity, and a slow shock. The compound wave is a discontinuity attached to a slow rarefaction, which can be attributed to the non strict hyperbolicity of the system (2.1)–(2.5). There is also a small Alfvén wave and a fast rarefaction going to the right, that are not shown in Figure 4.1. Figure 4.1 shows results from our 3-wave solver with the HLL solver. As expected, the 3-wave solver has much better resolution of the contact discontinuity. The 3-wave solver also strongly improves the sharpness of the slow shock and the compound wave. The fast waves are well resolved by both solvers. Figure 4.2 compares the 3-wave and 5-wave relaxation solvers. The 5-wave solver improves the resolution of the compound wave compared to the 3-wave solver.

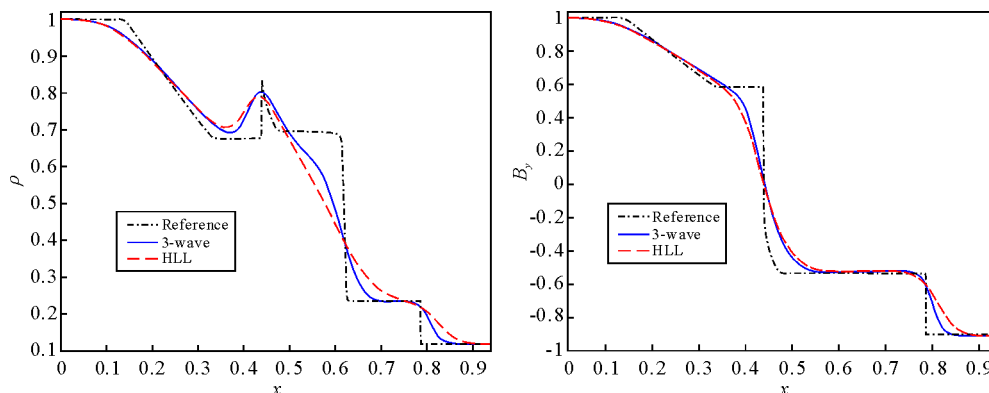


Fig. 4.1 ρ and B_y for Brio-Wu shock tube at time $t = 0.2$ with resolution $\Delta x = 0.01$.

The reference solution is a 3-wave simulation with $\Delta x = 0.0001$.

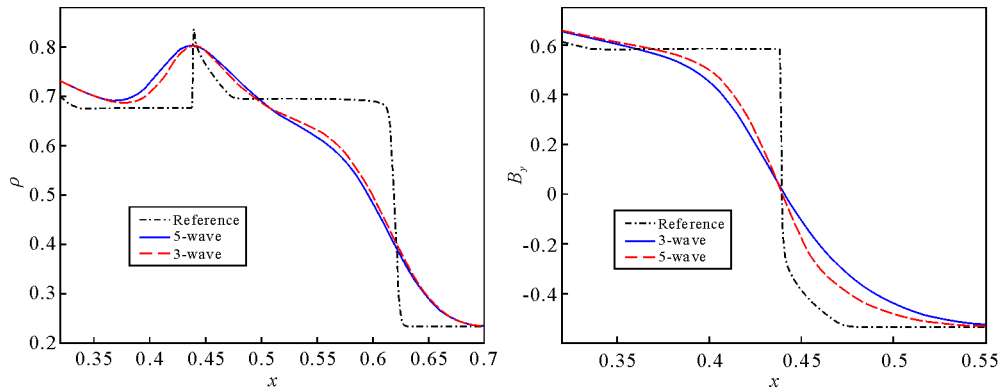


Fig. 4.2 ρ and B_y for Brio-Wu shock tube at time $t = 0.2$ with resolution $\Delta x = 0.01$. The reference solution is a 3-wave simulation with $\Delta x = 0.0001$. Note the different x -axis ranges.

4.2 Vacuum

A severe test for a scheme is the presence of vacuum in the initial data. It is crucial that the scheme preserves positivity. We test shock tube initial data given by $U = U_l$ for $x < 0.5$, and $U = U_r$ for $x > 0.5$, with $\gamma = 2$ and

$$\begin{aligned} \rho_l &= 0, \mathbf{u}_l = 0, \mathbf{B}_l = 0, p_l = 0, \\ \rho_r &= 1, \mathbf{u}_r = 0, \mathbf{B}_r = (0, 1, 0), p_r = 0.5. \end{aligned}$$

Figure 4.3 shows results with the 3-wave solver for the first and second order schemes. The standard second order scheme without the modification of Proposition 2.1 failed.

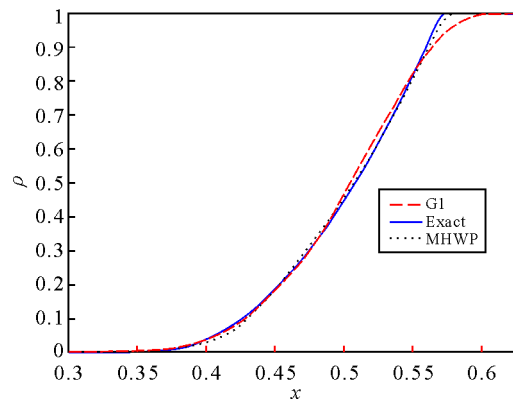


Fig. 4.3 Vacuum test as computed by first order scheme G1 and second order scheme MHWP. The exact solution can be found in [5]. The resolution was $h = 0.005$, and ρ is plotted at $t = 0.1$.

4.3 Isothermal blast wave

This two-dimensional test from [2] is sensitive to errors related to the treatment of $\nabla \cdot \mathbf{B}$, (see also [10]). It consists of a circular explosion in a moderately strong, homogenous magnetic field. The initial data were given by

$$\rho = 1, \mathbf{u} = 0, B_x = 5/\sqrt{\pi}, B_y = 0, B_z = 0,$$

except that in a circle of radius 0.05 we had $\rho = 100$. Pressure was determined by assuming isothermality throughout, i.e., $p = \kappa^2 \rho$, where the sound speed κ was set to 1. The isothermality

condition was enforced after every directional sweep. We compare our 3-wave solver based scheme with standard second order schemes based on a Roe solver and an HLLC solver as implemented in Flash 2.5. The latter two used a central discretisation of the Powell source term, which explains the spurious effects seen in Figure 4.4. Our scheme produces a clean approximation. Hence, we conclude that a proper upwind discretisation of the Powell term, such as presented here, is necessary.

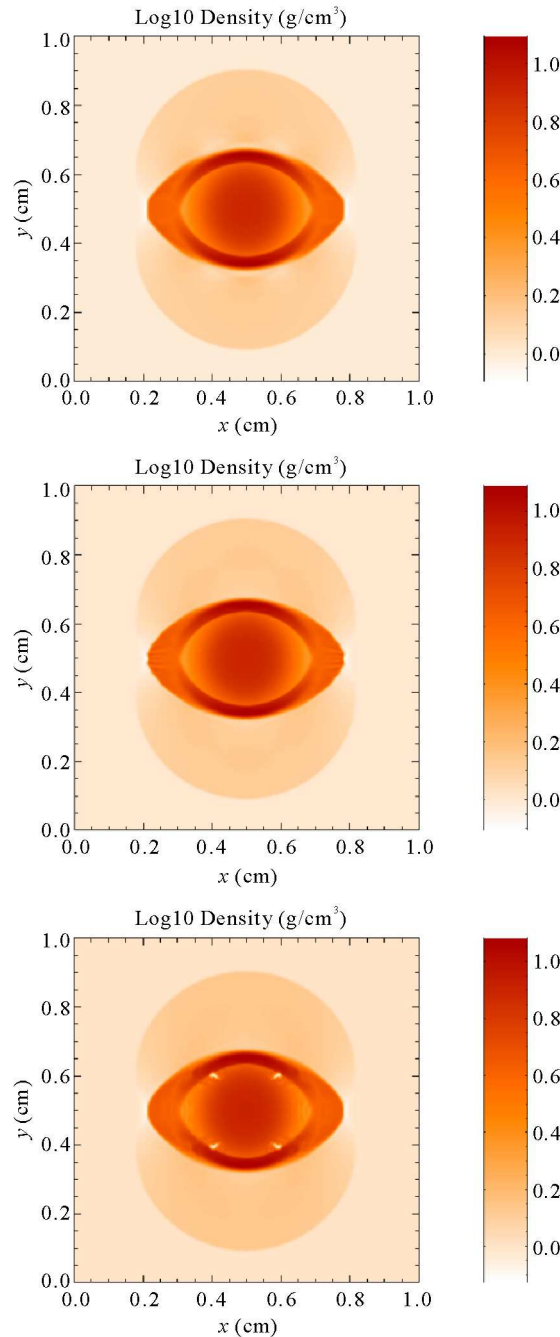


Fig. 4.4 Isothermal blast wave at time $t = 0.09$ with: Top to bottom: Flash 2.5 with our method, Flash 2.5 with Roe solver and Flash 2.5 with HLLC solver.

5 Outlook

In this paper we present a stable and accurate scheme for ideal MHD based on a relaxation approach. The scheme is of finite volume type with the following new elements: 1) Riemann solver: An HLL-type approximate Riemann solvers derived from relaxation that are entropy stable and positive, 2) Second order: A MUSCL-type reconstruction that preserves the positivity property of the Riemann solver, and 3) Multi-dimensions: A stable and natural upwind discretisation of the Powell source terms. All these ideas have been found crucial in obtaining the desired stability and accuracy. Nevertheless, they could be considered separately if desired.

The MUSCL-type reconstruction considered was restricted to second order. For some problems it is desirable to have a scheme that can resolve smooth regions to higher order. Hence, it would be of practical interest to extend our approach to higher order schemes. Another numerical issue of interest is the control of $\nabla \cdot \mathbf{B}$. The Powell method presented here is compatible with the 'divergence cleaning' techniques of [6], [14] and, to some extent, [8], with the disclaimer that proofs of stability are not available. In applications, there are often additional features in the equations such as source terms due to gravity, combustion, radiation etc. These features should be treated numerically such that the entropy stability and positivity properties are not violated. As an example, passively advected scalars can be added to the system following [3]. An important example of passively advected scalars could be mass fractions of different molecular species. The treatment of an external gravity field is discussed in [11].

References

- [1] Audusse Emmanuel, Bouchut François, Bristeau Marie-Odile, Klein Rupert, Perthame Benoît. A fast and stable well-balanced scheme with hydrostatic reconstruction for shallow water flows. *SIAM J Sci Comput*, 2004, **25**(6): 2050–2065
- [2] Balsara Dinshaw S, Spicer Daniel S. A staggered mesh algorithm using high order Godunov fluxes to ensure solenoidal magnetic fields in magnetohydrodynamic simulations. *J Comput Phys*, 1999. **149**(2): 270–292
- [3] Bouchut François. *Nonlinear Stability of Finite volume methods for hyperbolic conservation laws and well-balanced schemes for sources*. Frontiers in Mathematics. Basel: Birkhäuser, 2004
- [4] Bouchut François, Klingenberg Christian, Waagan Knut. A multiwave approximate Riemann solver for ideal MHD based on relaxation I - theoretical framework. *Numerische Mathematik*, 2007, **108**(1): 7–41
- [5] Bouchut François, Klingenberg Christian, Waagan Knut. A multiwave approximate Riemann solver for ideal MHD based on relaxation II - numerical implementation with 3 and 5 waves. To appear in *Numerische Mathematik*, 2010
- [6] Brackbill J U, Barnes D C. The effect of nonzero product of magnetic gradient and B on the numerical solution of the magnetohydrodynamic equations. *J Comput Phys*, 1980, **35**: 426–430
- [7] Brio M, Wu C C. An upwind differencing scheme for the equations of ideal magnetohydrodynamics. *J Comput Phys*, 1988, **75**(2): 400–422
- [8] Dedner A, Kemm F, Kröner D, Munz C -D, Schnitzer T, Wesenberg M. Hyperbolic divergence cleaning for the MHD equations. *J Comput Phys*, 2002, **175**(2): 645–673
- [9] Fryxell B, Olson K, Ricker P, Timmes F X, Zingale M, Lamb D Q, MacNeice P, Rosner R, Truran J W, Tufo H. Flash: An adaptive mesh hydrodynamics code for modeling astrophysical thermonuclear flashes. *The Astrophysical Journal Supplement Series*, 2000, **131**(1): 273–334
- [10] Fuchs F, McMurry A, Mishra S, Risebro N H, Waagan K. Approximate Riemann-solver based High-order Finite Volume schemes for the Godunov-Powell form of the ideal MHD equations in multi-dimensions. Submitted
- [11] Fuchs F, McMurry A, Mishra S, Risebro N H, Waagan K. Finite Volume Methods for Wave Propagation in Stratified Magneto-Atmospheres. *Commun Comput Phys*, 2010, **7**(3): 473–509

-
- [12] Harten A, Osher S, Engquist B, Chakravarthy S R. Some results on uniformly high-order accurate essentially nonoscillatory schemes. *Appl Numer Math*, 1986, **2**(3-5): 347–378
 - [13] Klingenberg Christian, Schmidt Wolfram, Waagan Knut. Numerical comparison of riemann solvers for astrophysical hydrodynamics. *J Comput Phys*, 2007, **227**(1): 12–35
 - [14] Marder Barry. A method for incorporating Gauss' law into electromagnetic pic codes. *J Comput Phys*, 1987, **68**(1): 48–55
 - [15] Powell Kenneth G. An approximate Riemann solver for magnetohydrodynamics (that works in more than one dimension). Technical report, Institute for Computer Applications in Science and Engineering (ICASE), 1994
 - [16] Shu Chi-Wang, Osher Stanley. Efficient implementation of essentially non-oscillatory shock-capturing schemes, ii. *J Comput Phys*, 1989, **83**(1): 32–78
 - [17] van Leer B. Towards the ultimate conservative difference scheme. V - A second-order sequel to Godunov's method. *J Comput Phys*, 1979, **32**: 101–136
 - [18] Waagan K. A positive MUSCL-Hancock scheme for ideal magnetohydrodynamics. *J Comput Phys*, 2009, **228**(23): 8609–8626
 - [19] Waagan Knut, Federrath Christoph, Klingenberg Christian. A robust code for astrophysical MHD. Preprint, 2010